International Journal of Nanotechnology and Applications
ISSN 0973-631X Volume 18, Number 1 (2024), pp. 1-16

https://dx.doi.org/10.37622/IJNA/18.1.2024.1-16

An Investigation on the Photodegradation Kinetics of Indigocarmine Dye and the Biological Activity of Electrochemically Synthesized Cds/Cus Nanoparticles as a Photo-Catalyst

K. M. Chaithra, H. S. Sindhushree and B. M. Venkatesha *
Department of Chemistry, Yuvaraja's College, University of Mysore, Mysuru, INDIA

Abstract

In the few decades use of nanostructured material have received a considerable importance because of its effective biological application, therefore nanostructured CdS/CuS nanocomposite photocatalyst synthesized by electrochemical method, which is a simple and an inexpensive method. The characterization techniques include are UV-visible spectroscopy, SEM-EDAX, and X-ray diffraction techniques. From UV-visible spectroscopy and by using tauc plot the band gap energy of CdS/CuS nanocomposite is calculated and is found to be 2.71eV. The SEM results shows surface of CdS/CuS includes some nano rod with cluster-like structure was observed. The EDAX spectra showed that the presence of cadmium, Sulphur and copper in the synthesized nanocomposite. From the XRD data and with the help of debye-scherrers formula the crystalline size is calculated and it is found to be 38.94nm. The photocatalytic activity of the synthesized CdS/CuS nanocomposite was examined by the kinetics of photodegradation of Indigocarmine dye. The degradation efficiency was found to be≈97%. The antimicrobial and anticancer activities were evaluated for the synthesized CdS/CuS nanocomposite against the control.

Keywords: Electrochemical method; CdS/CuS nanocomposite; Indigocarmine dye; antibacterial activity.

Introduction

Due to the potential to degrade environmental pollutants in an environmentally friendly way, heterogeneous photocatalysis has attracted considerable attention in recent years. Metal chalcogenides are promising candidates to be used as photocatalysts, since they possess excellent catalytic activity. Coupling CdS nanoparticles with other materials to form heterojunction structures is an effective method to promote the effective separation of photo generated electron-hole pairs and achieve high photocatalytic activity. Therefore, it is reasonable to deduce that

constructing CdS-CuS heterojunction could result in enhanced photocatalytic performance [1-3]. Semiconductor nanoparticles (NPs) are receiving extensive attention owing to their tunable chemical, optical, physical, and electrical properties. Semiconductor NPs with tunable bandgap, structure, and linear and nonlinear optical characteristics are excellent candidates for use in diverse applications ranging from energy harvesting, communication and information technology, biology, medicine, sensors, displays, illumination, and cameras [4-6].Semiconductor photocatalysis as a green technology for wastewater/organic contaminants treatment and green energy production has attracted considerable attention since Fujishima and Honda realized water splitting to generate hydrogen by using TiO_2 . Since then, various photocatalysts, such as transition metal oxides, metal sulphides, heterojunctions, doping materials, composite structures, have been synthesized to improve the photocatalytic activities. Among them, metal chalcogenides were considered to be promising photocatalytic candidates due to their unique properties, such as suitable band gap, ideal electronic band position and thus exhibiting excellent catalytic activities. [7-10]. Rapid industrial growth and urbanization of the population are causing pollution of the aquatic environment that needs to be addressed worldwide. Effluents from different industries, including textile, agriculture, leather, printing and paint, pharmaceutical, seafood, agrochemical, etc., Metal sulphides such as Bi_2S_3, CuS, ZnS, In_2S_3, CdS, Co_3S_4, Ag_2S have paid more attention due to their excellent photocatalytic performance under visible light irradiation and it is widely used for the wastewater treatment process. Among them, cadmium sulphide (CdS) is one of the emerging material and not only a visible light active photocatalyst, it is used in many fields such as optoelectronic devices, laser light emitting diodes, solar cells and photo detectors. However, the photocatalytic activity of CdS alone is limited, due to the fast recombination of photo induced charge carriers [11-15]. CdS has attracted much attention due to its conduction band position and band gaps being suitable for energy conversion under visible light. As is known, CdS is an important visible light photocatalyst because of its sensitivity to visible light irradiation and efficient photoexciton generation, which are excellent qualities for a photocatalyst. However, CdS has some disadvantages for further application. First, CdS nanostructures can easily aggregate during photocatalytic reactions, which can reduce the surface area. Second, the photoexciton recombination is ultrafast, and there is a lack of reactive sites [16-19]. Copper sulphide (hexagonal covellite, CuS) is a p-type semiconductor, that enables it to absorb a large fraction of the solar spectrum. In addition, a high concentration of charge carriers due to copper vacancies leads to plasmonic absorption in the infrared region. Thus, CuS nanostructures are of interest for photovoltaic and photocatalytic applications. The morphology, size, and surface area of CuS nanostructures control its photocatalytic efficiency. Porous nanostructures with a large active surface area are highly desired for catalytic applications [20-24]. Industrial effluents containing dyes pose a serious environmental hazard since their dumping into natural water bodies frequently results in environmental contamination, functioning as a source of non-aesthetic pollution, eutrophication, and so causing harm to aquatic life. The removal or degradation of stubborn synthetic dyes is a major ecological issue that is difficult to solve. Advanced oxidation processes (AOPs), a

promising technique, have recently been widely used for decolourization and degradation of textile dyes. The heterogeneous photocatalytic oxidation method is a technology that uses photocatalysts that is currently being investigated [25].

Materials and Methods

All chemicals were used to prepare CdS/CuS nanocomposite were the analytical grades of purity. Cd and Cu wire were purchased from Alfa Aesar. Indigocarmine dye from lobachemie, Platinum electrode from Elico pvt.ltd. All solutions were prepared in double distilled water. The optical properties for prepared CdS/CuS nanocomposite were studied by uv-visible spectrophotometer (shimadzu-1700 series). The x-ray crystallographic interpretations were performed by x-ray diffractometer (panalytical x-pert) using Cu Ka wavelength (λ=1.54 A°) scanning range from 0 to 70^0. The morphological feature for the prepared CdS/CuS nanocomposite study had determined by scanning electron microscopy (SEM-EDEX) from quanta-200 FEI, Netherlands. The elemental analysis for the conformation of prepared Cd, Cu and S is confirmed from energy dispersive X-ray analysis (EDAX).

Synthesis of CdS/CuS Nanocomposite by Electrochemical Method

Nanoscaled CdS/CuS nanocomposite was synthesized by an electrochemical process using Cd and Cu electrodes in an aqueous system with sodium sulphide as a conductive salt. The sodium sulphide was employed as the sulphur source. An electrochemical process based on an electrolytic cell was used. Platinum, Cd and Cu were used as electrodes with a lateral distance of 1.5 cm. They were fixed in a holder so that they were completely enclosed by the electrolyte. The Cd and Cu wires are used as anode and platinum electrode is used as cathode using 20mA current and potential of 15V the experiment was run for 2hrs with continuous stirring. The electrolytic cell is consisting of 0.2M of Na_2S solution. The electrochemically generated S^{2-} species reacted with Cd^{2+} and Cu^{2+} in the electrolyte to produce CdS/CuS nanocomposite shown in scheme-1. Finally, thus formed nanocomposite was washed repeatedly with distilled water until sodium sulphide is completely removed, centrifuged and calcinated at 750°C for 2 hr to remove sodium and hydroxide impurities which has formed due to electrolysis and atmospheric oxidation.

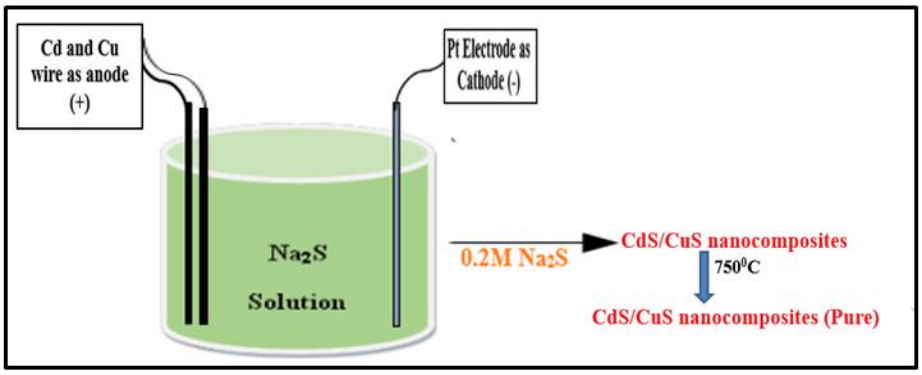

Figure 1. Experimental set up for the electrochemical synthesis of CdS/CuS nanocomposites

$$Cd \rightleftharpoons Cd^{2+} + 2e^-$$
$$Na_2S \longrightarrow 2Na^+ + S^{2-}$$
$$2Na^+ + 2e^- \longrightarrow 2Na \text{ (at Pt electrode)}$$
$$Cd^{2+} + S^{2-} \longrightarrow CdS$$

$$Cu \rightleftharpoons Cu^{2+} + 2e^-$$
$$Na_2S \longrightarrow 2Na^+ + S^{2-}$$
$$2Na^+ + 2e^- \longrightarrow 2Na \text{ (at Pt electrode)}$$
$$Cu^{2+} + S^{2-} \longrightarrow CuS$$

$$\text{The overall reaction is, } Cd \xrightarrow[Na_2S]{Cu} \text{CdS / CuS nanocomposites}$$

Scheme-1

Results and Discussion

UV-Visible Spectra

UV-Visible spectrum Figure 2(A) of CdS/CuS nanocomposites over the range 200-700 nm showed photoabsorption properties no longer than 349.68 nm, which suggest that the catalyst is photo active under UV light irradiation. Assuming the CdS/CuS solid as direct semiconductor and it is possible to calculate the band gap of CdS/CuS by constructing a Tauc plot [26,27]. The Tauc plot of nanocomposite is displayed in Figure 2(B). The energy of the band gap of CdS/CuS nanocomposite could be thus estimated to be 2.71 eV. It is reported that Cd loading results in enlarge surface area of the CdS/CuS photocatalyst. However, the increase of surface area is likely not the main factor affecting the photocatalytic activity of CdS/CuS.

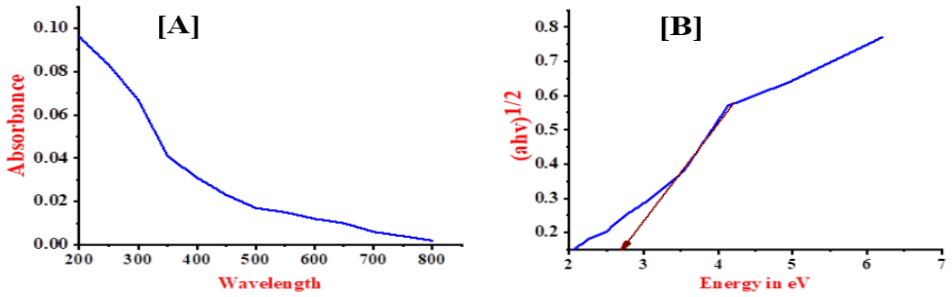

Figure 2. UV-Visible spectra (A) and Tauc plot (B) of CdS/CuS nanocomposite

X-Ray Diffraction

The XRD patterns of CdS/CuS nanocomposite figure 3(A) exhibit tetragonal crystal structure with similar peaks. The broadening of XRD peaks confirms nanocrystalline nature of the as prepared samples. The diffracted peaks obtained at diffraction angles 2θ of 18.25, 25.73, 27.80, 33.87, 35.49 41.88 and 48.71 corresponds to the (111), (102), (103), (006), (104), (004) and (110) planes of CdS/CuS peaks with cubic

structure. The crystallite size was calculated using Williamson-Hall (W-H) plot figure 3(B). W-H method reported that the XRD pattern broadening is attributed to both crystallite size and lattice strain. The XRD peak broadening due to micro strain is given by

$$\beta_\varepsilon = 4\varepsilon\tan\theta \quad (1)$$

Where β_ε is broadening due to strain, ε is the strain and θ is the peak position in radians.

$$\beta\cos\theta = k\lambda/D + 4\varepsilon\sin\theta \quad (2)$$

From equation (2) is Williamson-Hall equation and represents the uniform deformation model (UDM) by plotting 4sinθ along the x-axis and βcosθ along the y-axis and from the linear fit of the data, the crystalline size was estimated from the Y-intercept and it was found to be 38..94nm, and the strain 'ε' was estimated from the slope [28,29] and it was found to be 4.1563 x 10^{-4}.

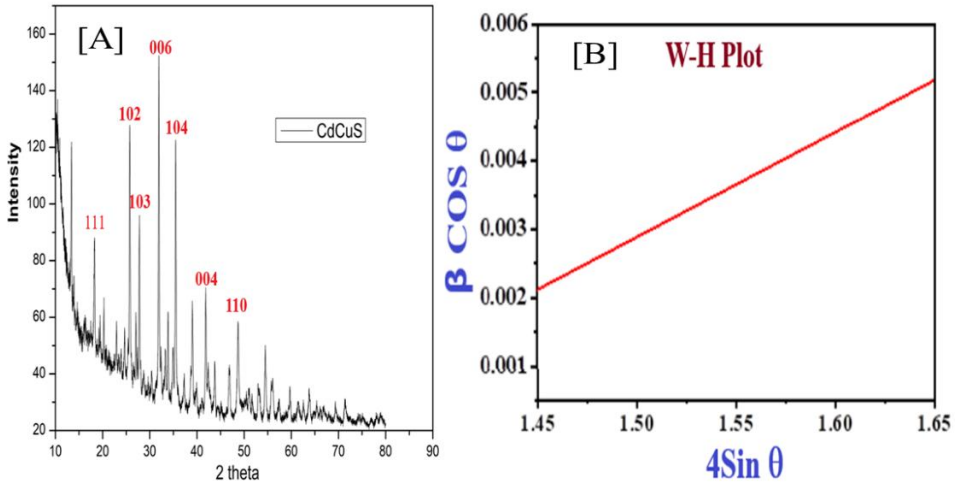

Figure 3. XRD patterns of CdS/CuS nanocomposite (A) and Williamson-Hall plot (B)

Scanning Electron Microscopy (SEM):

The morphology of CdS/CuS nanocomposite was investigated by FE-SEM shown in (Fig. 4). It can be found from the figure. 4 that the surface of CdS/CuS includes some nano rod with cluster-like structure were observed. From the EDAX analysis fig.5 The presence of Cd, Cu and sulphur were confirmed. Table1 indicates Quantitative Results for: Base (476)

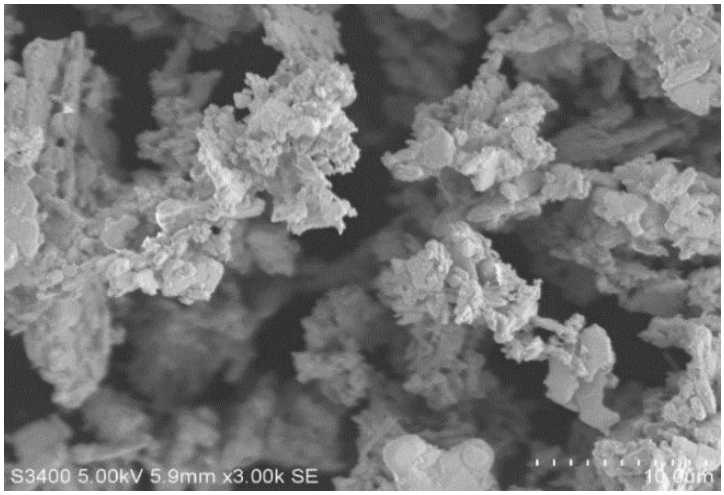

Figure 4.SEM images of electrochemically synthesized CdS/CuS nanocomposite

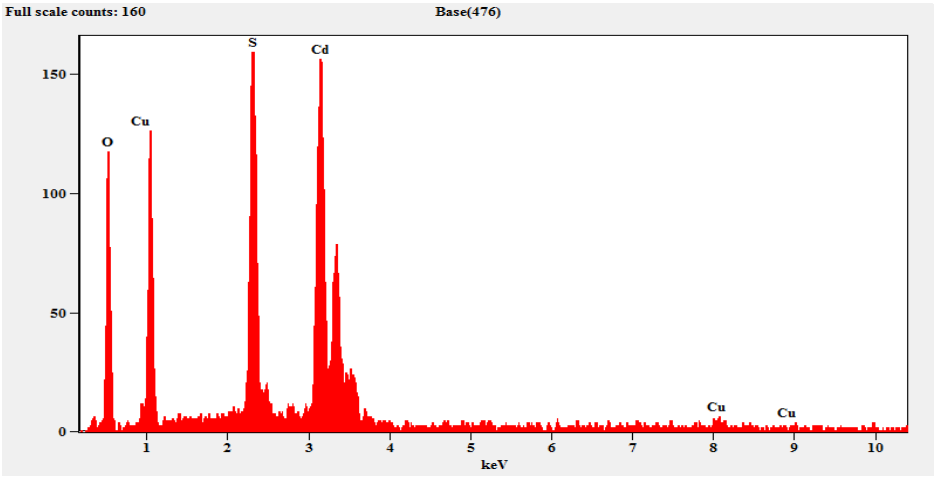

Figure 5: Energy dispersive X-ray analysis spectrum of electrochemically synthesized CdS/CuS nanocomposite

Table1: Quantitative Results for: Base (476)

Element Line	Weight %	Weight % Error	Atom %
O K	39.60	± 1.67	74.38
S K	12.79	± 0.51	11.99
S L	---	---	---
Cu K	4.41	± 1.26	2.08
Cu L	---	---	---
Cd L	43.20	± 2.17	11.55
Cd M	---	---	---
Total	100.00		100.00

FT-IR Spectra

The use of Fourier-transform infrared spectroscopy (FT-IR) to analyse the functional groups in CdS/CuS nanocomposites is a valuable technique for understanding the chemical composition of material. It's interesting to note the variations in vibration bands as the composition of the nanocomposites changes. Specifically, the absorption bands around 650 cm^{-1} are associated with CdS stretch vibrations, and their intensity decreases as the amount of CuS in the matrix increases. On the other hand, the bands between 530-683 cm^{-1}, typically present in CuS samples, correspond to Cu-S stretching bonds within the CuS lattice, and their intensity also decreases with higher CuS content in the CdS/CuS composites. Additionally, the band observed at 520-541 cm^{-1} is likely related to S-S bonds, and its intensity varies with the alloying parameter, suggesting changes in the nanocomposite's structure. Furthermore, you've identified the bending and stretching vibrations of sulphide molecules at 1098 and 1428cm^{-1}. This information from the FT-IR analysis contributes to a comprehensive characterization of your CdS/CuS nanocomposites.

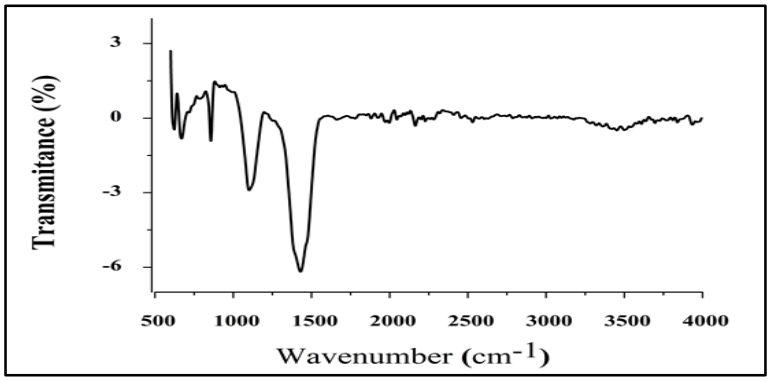

Figure 6: FTIR spectrum of CdS/CuS nanocomposites

Photodegradation Kinetics and COD Measurements

Effect of Concentration of Dye:

Degradation is carried out in different concentrations of dye (Table. 2). As the optimum catalyst concentration for CdS/CuS nanocomposite is 0.02g, keeping this as standard the same amount of CdS/CuS nanocomposite is taken for comparison in the further work. As the initial concentration of dye increases, the degradation efficiency reduces (Fig.7A). The possible reason is that, as initial concentration of dye is increased; more dye molecules are adsorbed onto the surface of the catalyst. but the adsorbed dye molecules are not degraded immediately because the intensity of the light and the catalyst amount is constant and also the light penetration is less. Also with the increase in the dye concentration, the solution becomes more intense coloured and the path length of the photons entering the solution is decreased thereby fewer photons reached the catalyst surface. Hence the production of hydroxyl and superoxide radicals are reduced. The COD for indigocarmine solution before and after degradation were measured (Fig.7B) and are given in Table 2. The pH before and after degradation has been reported. It is observed that after degradation the pH of the

dye solution is slightly decreased. The indigocarmine dye was found to have mineralized into H_2O, CO_2 and simpler inorganic salts (Scheme-2 and 3) [36], after being irradiated for 5 hrs using CdS/CuS photo catalysts. The Photodegradation efficiency of the photo catalyst was calculated by the following formula,

$$\text{Photodegradation efficiency} = \frac{\text{Initial COD} - \text{Final COD} \times 100}{\text{Initial COD}}$$

$$Np + h\gamma \longrightarrow e^- + h^+$$
$$h^+ + H_2O \longrightarrow OH^\bullet + h^+$$
$$h^+ + OH^- \longrightarrow OH^\bullet$$
$$e^- + O_2 \longrightarrow HO_2^\bullet + OH\bullet$$
$$HO_2^\bullet + H_2O \longrightarrow OH^\bullet + H_2O$$
$$H_2O_2 \longrightarrow 2\ OH^\bullet$$
$$OH^\bullet + IC \longrightarrow \text{Intermediate products}$$
$$O_2^{-\bullet} + IC \longrightarrow \text{Degradation products}$$
$$\longrightarrow CO_2, H_2O, NH_3 \text{ and other products}$$

Scheme-2

Table 2. Effect of concentration of Indigocarmine dye on rate of photodegradation under UV light
[CdS/CuS] =0.02gm/20ml, Temperature = 308K

10^{-5} [IC]	10^{-4} k Sec^{-1}	Time taken for 95% Degradation in min	Effect of pH		COD Values in mg/L	
			Before degradation	After degradation	Before degradation	After degradation
1.0	4.030	20	10.09	9.01	420	32
2.0	1.995	60	9.45	9.16	512	16
3.0	1.151	150	9.21	9.09	560	24
4.0	0.767	240	9.11	8.85	576	48

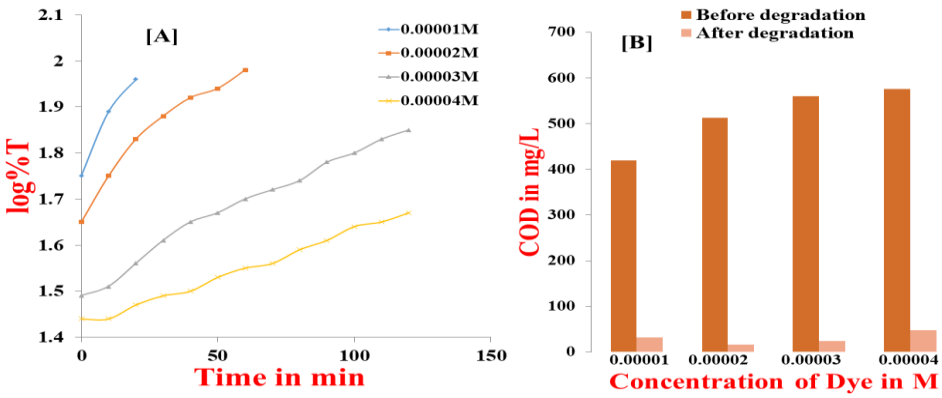

Figure 7: Effect of Concentration of Indigocarmine dye on rate of degradation(A) and COD Values of dye solution under UV light(B).

Effect of Catalyst Loading

Table 3 shows the rate constant of degradation with respect to different concentration of catalyst. Several studies have indicated that the photocatalytic rate initially increases with catalyst loading and then decreases at high values because of light scattering and screening effects. The tendency toward agglomeration (particle-particle interaction) also increases at high solids concentration, resulting in a reduction in surface area available for light absorption and hence a drop in photocatalytic degradation rate [37]. Although the number of active sites in solution will increase with catalyst loading, a point appears to be reached where light penetration is compromised because of excessive particle concentration. A further increase in catalyst loading beyond the optimum will result in non-uniform light intensity distribution, so that the reaction rate would indeed be lower with increased catalyst dosage. Further, the present study indicated, from economic point of view, the optimized photocatalyst loading is 0.02g/20 ml (Fig.8(A) and Table 3). The COD effect has been reported in Fig.8(B).

Table 3. Effect of catalyst loading on the photodegradation of Indigocarmine under UV light

[IC]=2x10^{-5} M, Temperature = 308K

Catalyst CdS/CuS in g	10^{-4}k Sec^{-1}	Effect of pH		COD Values in mg/L	
		Before degradation	After degradation	Before degradation	After degradation
0.01	1.573	9.61	9.46	512	32
0.02	1.995	9.45	9.16	512	16
0.03	2.840	9.32	8.86	512	16

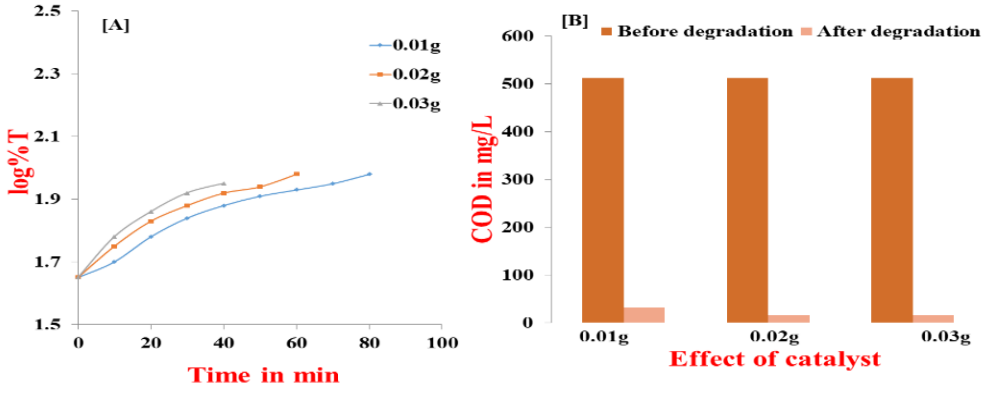

Figure 8: Effect of catalyst loading on the rate of degradation (A) and COD values of dye solution under UV light (B).

Effect of pH

The pH of the solution is one of the important factors in evaluating the Photo degradation reaction in aqueous medium. In the present study, the pH of the solution was adjusted by adding 0.01 M HCl solution and 0.01 M NaOH. The effect of pH was studied at pH 5.0, pH 7.30 and pH 9.5 by keeping all other experimental conditions constant. The results are reported in Fig.9(A) and Table 4. From the results it is observed that the rate of photodegradation increases from pH 5.0 to pH 9.5, the rate of degradation increases with increasing pH. Also, the amount of catalyst recovered after the experiment was lowered at lower pH because of the dissolution of the semiconductor sulphides at very low pH values. COD effects are reported in Fig.9(B). The optimum pH selected is 7.30 at which photodegradation is high.

Table 4. Effect of pH on photo degradation of Indigocarmine under UV light
[IC dye] = 2x10^{-5} M, [NP] = 0.02gm/20ml, Temperature = 308K

PH	10^{-4} k Sec^{-1}	COD Values in mg/L		Photodegradation Efficiency %
		Before degradation	After degradation	
5.0	1.189	512	24	95.31
7.30	1.995	512	16	96.87
9.5	2.379	512	48	90.62

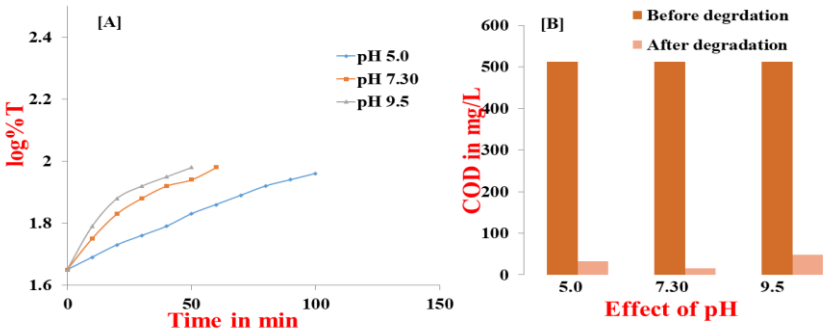

Figure 9: Effect of pH on the rate of degradation (A) and COD values of dye solution under UV light (B).

Effect of Temperature:

Temperature is one of the essential factors which effect on the rate of photo degradation. It is clear that the increase in temperature increases the degradation efficiency. Increase of temperature indicates increase in the rate of photodegradation as raise in temperature results in increase of number of effective collisions leading to higher rate of reaction (Fig.10A). However, the photodegradation efficiency is not much affected (Table 5). The rate constant and COD values are reported in table 5 and figure 10(B) and thermodynamic parameters were calculated and are reported in table 6.

Table 5. Effect of temperature on photo degradation of Indigocarmine under UV light
[IC dye] = 2x10^{-5} M, [NP] = 0.02gm/20ml

Temperature in K	10^{-4} k Sec^{-1}	COD Values in mg/L		Photodegradation Efficiency %
		Before degradation	After degradation	
298	1.151	512	16	96.87
308	1.995	512	16	96.87
318	3.070	512	48	95.31

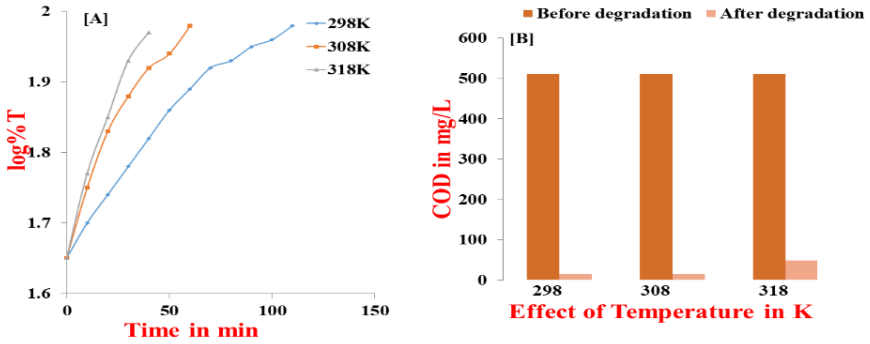

Figure 10: Effect of temperature on the rate of degradation (A) and COD values of dye solution under UV light (B).

Table 6: Thermodynamic parameters for indigocarmine dye

Temperature in K	ΔH# kJ/mol	ΔS# J/K/mol	ΔG# kJ/mol	Ea kJ/mol
298	36.40	-198.19	95.46	38.88
308	36.32	-198.11	97.33	
318	36.24	-198.78	99.45	

Effect of Light Intensity

The photodegradation rate for the degradation of IC with UV light is compared with sunlight. It is observed that the photodegradation rate is high in UV light for prepared photocatalyst compared to sunlight (Table 8). The reason is that, the inclusion of Cu^{2+} in CdS matrix caused an increase in the band gap of CdS from 2.39 eV to 3.26 eV, indicating that these semiconductor nanoparticles absorb UV light. This can subsequently activate these modified metal sulphide photocatalysts upon UV light irradiation. When a photon incident on a semiconductor (CdS/CuS) has energy that matches or exceeds the band gap energy of the semiconductor, an e^- is promoted from the valence band (VB) into the conduction band (CB), leaving a hole in the VB. Excited-state CB electrons and VB holes can recombine and dissipate the input energy as heat, get trapped in metastable surface states, or react, respectively, with electron acceptors and donors that happen to be adsorbed on the semiconductor surface or within the surrounding electrical double layer of the charged nanoparticles. In the absence of suitable e−/h+ scavengers the stored energy is dissipated within a

few nanoseconds by recombination. If a suitable scavenger or surface defect state is available to trap the electron or hole, recombination is prevented and subsequent redox reactions may occur. As the number of defects in CdS/CuS nanocomposite, electron or hole recombination is prevented and therefore the CdS/CuS is very active under UV light compared to sunlight.

Table 7: Effect of rate of degradation in sunlight and UV light

Catalyst 0.02g	**Concentration of Indigocarmine in M**	**Sun Light 10^4 k Sec-1**	**Time taken for 95% degradation in min**	**UV light 10^4 k Sec^{-1}**	**Time taken for 95% degradation in min**
CdS/CuS nanocomposite	$2x10^{-5}$	0.191	480	1.995	60

Degradation Pathway of Indigocarmine Dye

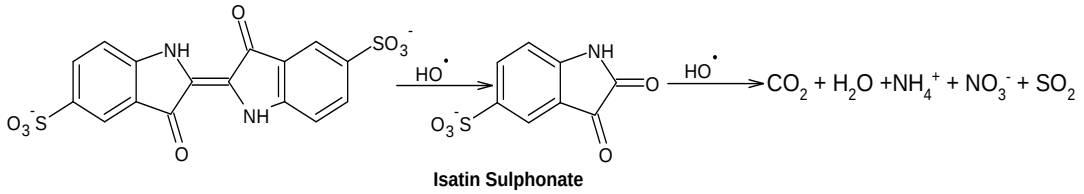

Scheme-3

Reusability and Regeneration

The re-use sample has shown almost same degradation efficiency compared to the fresh samples. This indicates the nano samples can be regenerated and re-used with very low or insignificant change in the efficiency. While an obviously decrease in rate of reaction was noticed with the second use of catalyst (Table.4). Reuse cycles might cause the aggregation of photo catalyst and the decrease in specific surface area and the losses of catalyst, resulting in a loss of catalytic activity.

Antibacterial Assay

Antibacterial Activity by Disc Diffusion Method

The test strain *Bacillus subtilis* (MTCC 441), *Lactobacillus acidophilus* (MTCC 447) and *Staphylococcus aureus* (MTCC 96) was obtained from The Microbial Type Culture Collection and Gene Bank (MTCC), Institute of Microbial Technology (IMTECH), Chandigarh, India. The antimicrobial activity was determined by disc diffusion methods (Kirby *et al*., 1966) in accordance with CLSI (2012) with slight modifications. About 25 mL of molten Mueller Hinton Agar was poured into a sterile Petri plate (Himedia, Mumbai, India). The plates were allowed to solidify, after which 18 h grown (OD adjusted 0.6)100 µl of above said type strains were transferred onto plate and made culture lawn by using sterile cotton swabs spreader. After five min setting of the test strains, test samples loaded onto with different concentrations (0µg/ml, 250µg/ml, 500µg/ml and 750µg/ml and 1000µg/ml) of test drug. The

azithromycin (30 µg/ml) served as a positive control. Discs were placed onto the plate between 24 mm diameter. The plain disc and commercial drug loaded (30 µg/mL) served as negative and positive controls, respectively. The plates were incubated at 37°C in a bacteriological incubator for 24 h. The antibacterial activity was determined by measuring the diameter of the zone of inhibition around the well using antibiotic zone scale (Himedia, Mumbai, India).

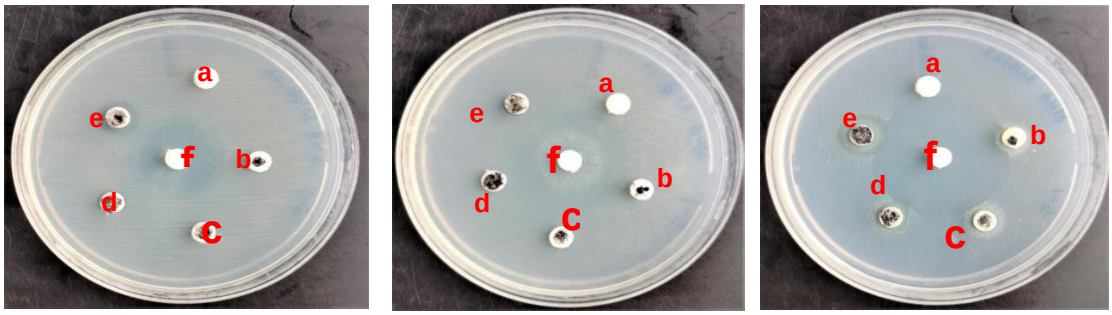

Bacillus subtilis Lactobacillus acidophilus Staphylococcus aureus

a: 0 µg/mL; b: 250 µg/mL; c: 500 µg/mL; d: 750 µg/mL; e: 1000 µg/mL; f: Azithromycin (30 µg/mL)

Figure 11: Antibacterial activity of sample CdS/CuS

Table 8: Antibacterial activity of CdS/CuS nanocomposites

Name of the Sample	**Zone of Inhibition (mm)**					**ZOI(mm) Standard***
	0 µg/mL	**250 µg/mL**	**500 µg/mL**	**750 µg/mL**	**1000 µg/mL**	**30 µg/well**
Bacillus subtilis	-	7	8	9	11	25
Lactobacillus acidophilus	-	9	10	11	12	27
Staphylococcus Aureus	-	10	12	14	15	24

Conclusion

Electrochemical method has shown good prospects in the controllable synthesis of small-sized Nano materials. Moreover, the obtained particles have highly enhanced photocatalytic activity. Therefore, the simple, cost-effective, and eco-friendly synthetic method allows for its application in large scale production. The kinetics of photo degradation of dye shows that at 0.02g of catalyst, CdS/CuS acts as an efficient photo catalyst in UV light. Kinetics of photodegradation of indigocarmine recommended that the degradation follows 1st order kinetics. The photodegradation rate is low in sunlight when compare to UV light, hence the synthesized CdS/CuS nanocomposite acts as a very good photocatalyst and is active under UV light. The complete degradation of dye solution was confirmed by COD measurement. The COD values revealed that 96% of the acid had been degraded. The synthesized

nanoparticles show appreciably good inactivation of different strains of bacteria. CdS/CuS Nanocomposite can be used for industrial waste water treatment and as an antibacterial powder.

Acknowledgements
The authors are grateful to late Prof.S. Ananda, former Professor and chairman, UGC – BSR faculty fellow, DOS in Chemistry, Manasagangothri, University of Mysore, Mysuru, for his keen encouragement and timely guidance, and also authors are acknowledges Yuvaraja's college, IOE, UPE & CPEPA, University of Mysore.

References

[1] Cds Nanoparticle-Decorated Cus Microflower-2d Graphene Hybrids and Their Enhanced Photocatalytic Performance. Z. G. Li,* , B. Zeng, Chalcogenide Letters, Vol. 18, No. 1, January 2021, P. 39 – 46
[2] M. A. Pandit, S. Billakanti, K. Muralidharan. J. Environ. Chem. Eng. 8(2), 103542 (2020).
[3] L. F. Luo, Y. D. Wang, S. P. Huo Et Al. Inter. J. Hydrogen Energy 44(59), 30965 (2019).
[4] Chemical bath synthesis of Ag2S, CuS, and CdS nanoparticle-polymer nanocomposites: structural, linear, and nonlinear optical characteristics. ALI FATEMI et al,Optical Materials Express Vol. 12, No. 7, 1 Jul 2022,2697-2710
[5] García de Arquer FP, DV Talapin, VI Klimov, Y Arakawa, M Bayer, and EH Sargent, "Semiconductor quantum dots: Technological progress and future challenges," Science 373(6555), eaaz8541 (2021).
[6] Y. Pu, F. Cai, D. Wang, J.-X. Wang, and J.-F. Chen, "Colloidal synthesis of semiconductor quantum dots toward large-scale production: a review," Ind. Eng. Chem. Res. 57(6), 1790–1802 (2018).
[7] One-pot hydrothermal synthesis of CdS decorated CuS microflowerlike structures for enhanced photocatalytic properties. Xiaolong Deng, Scientific Reports | 7: 3877 | DOI:10.1038/s41598-017-04270-y
[8] Chen, X. et al. Facile fabrication of novel porous graphitic carbon nitride/copper sulfide nanocomposites with enhanced visible light driven photocatalytic performance. J. Colloid Interf. Sci. 476, 132–143 (2016).
[9] Kriegel, I. et al. Tuning the excitonic and plasmonic properties of copper chalcogenide nanocrystals. J. Am. Chem. Soc. 134, 1583–1590 (2012)
[10] He, W. et al. Flexible and high energy density asymmetrical supercapacitors based on core/shell conducting polymer nanowires/ manganese dioxide nanoflakes. Nano Energy 35, 242–250 (2017).
[11] Synthesis and Characterization of CuS/CdS Photocatalyst with Enhanced Visible Light-Photocatalytic Activity. A. Malathi1 et al, Journal of Nano Research, ISSN: 1661-9897, Vol. 48, pp 49-61.
[12] R. Dhanabal, A. Chithambararaj, S. Velmathi, A. Chandra Bose, Visible light driven degradation of methylene blue dye using Ag3PO4, J. Environ. Chem. Eng. 3 (2015) 1872- 1881.
[13] F. Jiang, T. Yan, H. Chen, A. Sun, C. Xu, X. Wang, A g-C3N4-CdS composite

catalyst with high visible-light-driven catalytic activity and photostability for methylene blue degradation, Appl. Surf. Sci. 295 (2014) 164-172.

[14] Synthesis, growth mechanism and photocatalytic H_2 evolution of CdS/CuS composite via hydrothermal method. Xiande Yang et al, RSC Adv., 2019, 9, 25142–25150

[15] Q. Li, B. D. Guo, J. G. Yu, J. R. Ran and B. H. Zhang, Highly Efficient Visible-Light-Driven Photocatalytic Hydrogen Production of CdS-Cluster-Decorated Graphene Nanosheets, J. Am. Chem. Soc., 2011, 133, 10878–10884.

[16] N. Zhang, S. Liu, X. Fu and Y. J. Xu, Fabrication of Coenocytic Pd@CdS Nanocomposite as a Visible Light Photocatalyst for Selective Transformation under Mild Conditions, J. Mater. Chem., 2012, 22, 5042–5052.

[17] W. Jiang, Y. Liu, R. Zong, Z. Li, W. Yao and Y. Zhu, Photocatalytic Hydrogen Generation on Bifunctional Ternary Heterostructured In2S3/MoS2/CdS Composites with High Activity and Stability under Visible Light Irradiation, J. Mater. Chem. A, 2015, 3, 18406–18412.

[18] Microwave-Assisted Synthesis of Porous Aggregates of CuS Nanoparticles for Sunlight Photocatalysis. C. Nethravathi,et al, ACS Omega 2019, 4, 4825−4831

[19] van der Stam, W.; Gudjonsdottir, S.; Evers, W. H.; Houtepen, A. J. Switching between Plasmonic and Fluorescent Copper Sulfide Nanocrystals. J. Am. Chem. Soc. 2017, 139, 13208−13217.

[20] Liu, Y.; Liu, M.; Swihart, M. T. Reversible Crystal Phase Interconversion between Covellite CuS and High Chalcocite Cu2S Nanocrystals. Chem. Mater. 2017, 29, 4783−4791.

[21] Yang, X.-Y.; Chen, L.-H.; Li, Y.; Rooke, J. C.; Sanchez, C.; Su, B.-L. Hierarchically Porous Materials: Synthesis Strategies and Structure Design. Chem. Soc. Rev. 2017, 46, 481−558.

[22] Petkovich, N. D.; Stein, A. Controlling Macro and Mesostructures with Hierarchical Porosity through Combined Hard and Soft Templating. Chem. Soc. Rev. 2013, 42, 3721−3739

[23] UV-light-driven cadmium sulphide (CdS) nanocatalysts: synthesis, characterization, therapeutic and environmental applications; kinetics and thermodynamic study of photocatalytic degradation of Eosin B and Methyl Green dyes. Sundas Ali et al, Water Science & Technology Vol 85 No 4, 1041-1052

[24] High Efficient Photocatalytic Degradation of 3,7-Bis(Dimethylamino)-Phenothiazin-5-Ium Chloride Dye and Kinetics of H_2 Evolution of $N_2H_4H_2O$ by Synthesized CdS/NiS Nanocomposite by Electrochemical Method. R. Shilpa, H. C. Charan Kumar, Sanniaha Ananda. Modern Research in Catalysis, 2021, 10, 15-35

[25] Belever, C., Adán, C. and Fernández-García, M. (2009) Photocatalytic Behaviour of Bi_2MO_6 Polymetalates for Rhodamine B Degradation. Catalysis Today, 143, 274-281

[26] Nasir, J.A., et al. (2018) Photocatalytic Dehydrogenation of Formic Acid on CdS Nanorods through Ni and Co Redox Mediation under Mild Conditions. ChemSusChem, 11, 2587-2592.

[27] Abd El-Sadek, M.S., et al. (2019) X-Ray Peak Profile Analysis and Optical Properties of CdS Nanoparticles Synthesized via the Hydrothermal Method. Applied Physics A, 125, 283
[28] F. Li, Y. Zhao, Q. Wang, X. Wang, Y. Hao, R. Liu, D. Zhao, Enhanced visible-light photocatalytic activity of active Al2O3/g-C3N4 heterojunctions synthesized via surface hydroxyl modification, J. Hazard. Mater. 283 (2015) 371-381
[29] X. Liu, Y. Yan, Z. Da, W. Shi, C. Ma, P. Lv, Y. Tang, G. Yao, Y. Wu, P. Huo, Y. Yan, Significantly enhanced photocatalytic performance of CdS coupled WO3 nanosheets and the mechanism study, Chem. Eng. J. 241 (2014) 243-250.
[30] Zein K. Heiba et al. Infuence of alloying ratio in tailoring the structural and optical properties of (1−x)CdS–xCuS nanocomposite. Applied Physics A (2020) 126:518. https://doi.org/10.1007/s00339-020-03700-5
[31] T.P. Martin, H. Schaber, Spectrochem. Acta A 38, 655 (1982)
[32] Y. Wang, L. Zhang, H. Jiu, N. Lia, Y. Sun, Appl. Surf. Sci. 303, 54 (2014)
[33] T.P. Martin, H. Schaber, Spectmchim. Acta A 38(6), 655 (1982)
[34] M.N. Kalasad, M.K. Rabinal, B.G. Mulimani, G.S. Avadhani, Semicond. Sci. Technol. 23(045009), 1 (2008)
[35] G.T. Rao, R.J. Stella, B. Babu, K. Ravindranadh, C.V. Reddy, J. Shim, R.V.S.S.N. Ravikumar, Mater. Sci. Eng., B 201, 72 (2015)
[36] Rakesh, Sannaiah Ananda, Netkal M. Made Gowda, Kithanakere Ramesh Raksha, Synthesis of niobium doped ZnO nanoparticles by electrochemical method: characterization, photodegradation of indigo carmine dye and antibacterial study, Adv. Nanopart. 3 (2014) 133-147.
[37] A K Subramani, K Byrappa, S Ananda, K M Lokanatha Rai C Ranganathaiah And M Yoshimura, *Bull. Mater. Sci.*, 2007, 30(10), 37–41